DEVELOPMENTAL DYNAMICS 245:844–853, 2016
DOI: 10.1002/DVDY.24412

A GAL4-inducible Transgenic Tool Kit for the In Vivo Modulation of Rho GTPase Activity in Zebrafish

Nicholas J. Hanovice,[1,2,*] Emily McMains,[1,*] and Jeffrey M. Gross[1,2*]

[1]Department of Molecular Biosciences, Institute for Cellular and Molecular Biology, The University of Texas at Austin, Austin Texas
[2]Department of Ophthalmology, Louis J. Fox Center for Vision Restoration, University of Pittsburgh School of Medicine, Pittsburgh Pennsylvania

Background: Rho GTPases are small monomeric G-proteins that play key roles in many cellular processes. Due to Rho GTPases' widespread expression and broad functions, analyses of their function during late development require tissue-specific modulation of activity. The GAL4/UAS system provides an excellent tool for investigating the function of Rho GTPases in vivo. With this in mind, we created a transgenic tool kit enabling spatial and temporal modulation of Rho GTPase activity in zebrafish. **Results:** Transgenic constructs were assembled driving dominant-negative, constitutively active, and wild-type versions of Cdc42, RhoA, and Rac1 under 10XUAS control. The self-cleaving viral peptide F2A was utilized to allow bicistronic expression of a fluorescent reporter and Rho GTPase. Global heat shock of *hsp70l*:gal4^{+} transgenic embryos confirmed GAL4-specific construct expression. Western blot analysis indicated myc-tagged Rho GTPases were expressed only in the presence of GAL4. Construct expression was confined to proper cells when combined with *pou4f3*:gal4 or *ptf1a*:gal4. Finally, transgene expression resulted in reproducible defects in lens formation, indicating that the transgenes are functional in vivo. **Conclusions:** We generated and validated 10 transgenic lines, creating a versatile tool kit for the temporal-spatial modulation of Cdc42, RhoA, and Rac1 activity in vivo. These lines will enable systematic analysis of Rho GTPase function in any tissue of interest. *Developmental Dynamics 245:844–853, 2016*. © 2016 Wiley Periodicals, Inc.

Key words: Cdc42; Rac1; RhoA; GAL4/UAS; zebrafish

Submitted 4 November 2015; First Decision 21 March 2016; Accepted 29 March 2016; Published online 22 April 2016

Introduction

Rho GTPases, a subfamily of Ras GTPases, are small monomeric G-proteins that play key roles in myriad cellular processes, including cell cycle progression, cytoskeletal dynamics, cellular polarity, and membrane trafficking (Etienne-Manneville and Hall, 2002; Takai et al., 2001). Rho GTPase activity depends upon a binary molecular switch: when bound to GTP, Rho GTPases are active; when bound to GDP, they are inactive. This switch is tightly regulated within the cell (Boguski and McCormick, 1993; Jaffe and Hall, 2005), as Rho proteins regulate numerous downstream processes through their interactions with a diverse array of effector proteins. Most studies of Rho GTPases have focused on the Rho subfamily proteins: Cdc42, Rac1, and RhoA. Cdc42 was first discovered in *Saccharomyces cerevisiae* as a protein required for proper cell polarity during budding (Adams et al., 1990). Since its discovery, Cdc42 has been shown to regulate membrane trafficking, actin filament polymerization to form filopodia, and numerous other cellular processes (Erickson and Cerione, 2001). Rac1 stimulates the assembly of lamellipodia and mediates the formation of cell adhesion structures (Bosco et al., 2009; Ridley et al., 1992). RhoA activity leads to the formation of actin stress fibers (Hall, 1998), maturation of focal adhesions (Luo, 2002), and contraction of the cytokinesis furrow (Lai et al., 2005; Piekny et al., 2005). All three proteins are required for cell cycle progression (Olson et al., 1995). Rho GTPases are also thought to be involved in diverse developmental and pathological processes, including axon pathfinding (Bashaw and Klein, 2010; Jin et al., 2005), cell migration (Kardash et al., 2010; Raftopoulou and Hall, 2004), and oncogenesis (Ellenbroek and Collard, 2007; Sahai and Marshall, 2002).

However, these analyses have predominantly utilized cell culture or in vitro methods, limiting insight into how Rho GTPases function in vivo. Indeed, in vivo investigations of the molecular functions of Rho GTPases during animal development have been relatively rare, owing to the need for tissue-specific approaches to manipulate their activity. For example, knockout of Cdc42 (Chen et al., 2000) or Rac1 (Sugihara et al., 1998) in mice results in severe pleiotropic defects and early embryonic lethality. Analysis of Rho GTPase activity and function in vivo therefore requires experimental approaches that allow modulation of activity in specific tissues or cell populations, and at specific time points (Chew et al., 2014; Govek et al., 2005; Heasman and Ridley, 2008; Heynen et al., 2013; Jackson et al., 2011; Luo et al., 1996; Ruchhoeft and Ohnuma, 1999; Wong and Faulkner-Jones, 2000; Xiang and Vanhoutte, 2011).

*Correspondence to: Jeffrey M. Gross, 3501 Fifth Avenue, BST3-2051 Pittsburgh PA, 15213; 412-383-7325. E-mail: grossjm@pitt.edu
*Nicholas Hanovice and Emily McMains indicating they have contributed equally to this work.

Article is online at: http://onlinelibrary.wiley.com/doi/10.1002/dvdy.24412/abstract

Zebrafish provide an excellent model for investigation of the molecular function of vertebrate Rho GTPases in vivo (Kardash et al., 2010; Lai et al., 2005; Salas-Vidal et al., 2005; Zhu et al., 2006). Previous studies of Rho GTPase function in developing zebrafish employed microinjection of mRNA to drive global overexpression of wild-type, constitutively active, or dominant negative versions (Hsu et al., 2012; Xu et al., 2014; Yeh et al., 2011; Zhu et al., 2008, Zhu et al, 2006), or morpholino oligos for transient disruption of Rho GTPase expression (Hsu et al., 2012; Srinivas et al., 2007). Due to the central role of Rho GTPases in early embryogenesis, approaches that modulate global Rho GTPase activity must focus on events occurring very early during zebrafish development, and thus have not been effective in analyzing the functions of these proteins during later developmental events. Following the development of highly efficient transgenesis techniques in zebrafish (Kwan et al., 2007), transgenic lines have been generated in which the expression of constitutively active and dominant negative versions of different Rho GTPase family members is driven by cell-type-specific promoters (Chew et al., 2014; Choe et al., 2013; Jung and Leem, 2013). Although these tools restrict Rho GTPase construct expression to specific cell and tissue types and, dependent on the promoter, allow functional investigations at later stages in development, systematic comparisons of functional roles of different Rho GTPase members in different tissues is limited to a small number of extant cell-type-specific promoter Rho GTPase transgenic lines (Chew et al., 2014; Choe et al., 2013; Jung and Leem, 2013). Moreover, this strategy necessitates the generation and validation of a new line for each desired promoter and/or Rho GTPase combination, an inefficient and time-consuming approach. The GAL4/UAS system is a powerful transgenic system for enabling the temporal-spatial control of transgene expression (Brand and Perrimon, 1993; Fischer et al., 1988; Ornitz et al., 1991; Scheer, 1999). In this system, a promoter fragment drives expression of the yeast transcription factor GAL4. GAL4 then binds an upstream activating sequence (UAS) to drive transgene expression. Gal4/UAS is widely used in zebrafish, and there are now hundreds of published GAL4 drivers and UAS constructs listed on www.zfin.org. The strength of this system lies in its flexibility: A single GAL4 transgene can be used to drive expression of multiple UAS constructs, enabling researchers to express multiple transgenes within a defined cellular or tissue context.

Taking advantage of this approach, we have created a versatile transgenic tool kit that enables spatial and temporal modulation of Rho GTPase activity in zebrafish. We generated and validated 10 GAL4-inducible transgenic lines that express dominant negative, constitutively active, and wild-type versions of Cdc42, RhoA, and Rac1, as well as a fluorescent protein marker to highlight expressing cells. We have confirmed GAL4-specific expression of these transgenes and have demonstrated transgene functionality by reporting reproducible lens phenotypes in induced embryos. These lines now enable systematic tissue-specific investigation of the molecular function of Rho GTPases in vivo.

Results and Discussion

Generation of GAL4-inducible Rho GTPase Transgenic Lines

To generate transgenic lines for GAL4-driven expression of Rho GTPases, we first designed and assembled transgenic constructs encoding wild-type (WT), dominant negative (DN), and constitutively active (CA) human Cdc42, RhoA, and Rac1 (Fig. 1). An additional DN Cdc42 was generated using *Xenopus* $Cdc42^{F37A}$, which has recently been utilized in vivo (Kieserman and Wallingford, 2009) and is 98% identical to human Cdc42. We selected the 10X UAS element (Kwan et al., 2007) for our constructs due to this promoter's strong GAL4-specific expression (Gabriel et al., 2012; Kwan et al., 2007). Although recent research has raised concern over multigenerational silencing of the repeat-heavy UAS element (Akitake et al., 2011; Goll et al., 2009), other reports have postulated that silencing may be reduced when UAS lines are maintained separately from GAL4 drivers (Choe et al., 2012). Cdc42 and RhoA constructs were assembled with the monomeric and highly photostable mCherry fluorescent protein (Shaner et al., 2004), while enhanced green fluorescent protein (EGFP) was chosen as the fluorescent reporter for Rac1 transgenics. A myc-tag was also added to enable detection of each Cdc42 and RhoA isoform, and there is a significant amount of literature reporting the use and effective function of C-terminal tags of Rho GTPases (Choe et al., 2012; Disanza et al., 2006; Hussain et al., 2001; Kim et al., 2008; Kroschewski et al., 1999; Lee et al., 2004; Sakurai-Yageta et al., 2008). Furthermore, our constructs were engineered using cDNAs that have been shown to be expressed and functional (Kieserman and Wallingford, 2009; Nobes and Hall, 1995). Nucleotide sequence encoding the self-cleaving viral peptide F2A was inserted between fluorescent reporters and Rho GTPase cDNA sequences to allow bicistronic expression of the fluorescent protein and the GTPase. Rather than requiring a second ribosomal binding event, as is the case for an internal ribosome entry site (IRES), F2A peptides lead to two protein products via a ribosomal skipping mechanism (Donnelly and Luke, 2001; Szymczak et al., 2004); and when compared to IRES, F2A leads to more efficient bicistronic expression (Chan et al., 2011; Wang et al., 2011). With this rationale, we created three types of constructs: 10x*uas*:mCherry-F2A-myc-$Cdc42^{XX}$ for the expression of mCherry-F2A and myc-Cdc42; 10x*uas*:EGFP-F2A-$Rac1^{XX}$ to express EGFP-F2A and Rac1; and 10x*uas*:mCherry-F2A-myc-$RhoA^{XX}$, to express mCherry-F2A and myc-RhoA (Fig. 1A). In all, we created a total of 10 new transgenic constructs as elaborated in Figure 1B. All constructs include the *cmlc2*:egfp transgenesis marker to allow easy visualization of the presence of constructs. Germ line transmission, scored by the appearance of offspring with ubiquitously GFP-positive hearts, occurred in outcrosses of roughly 25% of injected F0 fish.

To determine the spatial expression of F1 alleles while minimizing the potential for severe phenotypes arising from early induction, we crossed F0 adults with *hsp70l:gal4* zebrafish, globally heat-shocked all transgenic embryos at ~54 hours post-fertilization (hpf), and imaged reporter expression at 72 hpf. Each line displayed robust and ubiquitous transgene expression following global heat shock (data not shown). No leakiness of transgene expression was observed before heat shock. Polymerase chain reaction (PCR) genotyping confirmed that fluorescent marker–positive embryos were also GAL4-positive, and non-fluorescent embryos were GAL4-negative (data not shown), indicating that UAS-driven transgene expression was restricted to fish expressing GAL4, and that there was no observable leaky activation of the UAS promoter.

Validation of Transgene Expression and GAL4 Sensitivity

Non-equimolar expression of the second cistron following F2A ribosomal skipping has been reported (Chan et al., 2011). Because

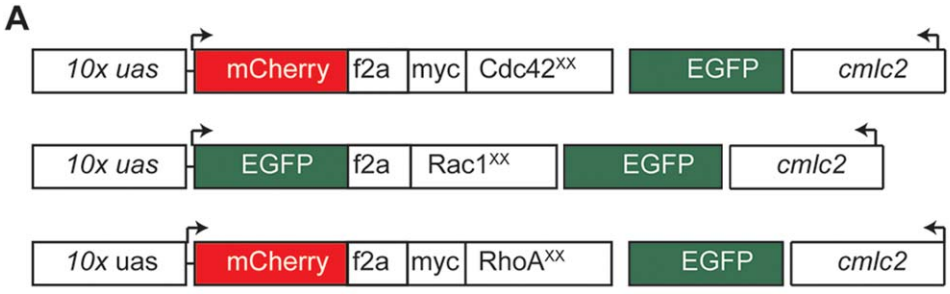

B

Allele	Construct	Mutation	Activity	Species
au66	*uas*:mCherry-F2A-myc-Cdc42^{WT}	———	Normal	Human
au68	*uas*:mCherry-F2A-myc-Cdc42^{CA}	Q61L	↑	Human
au67	*uas*:mCherry-F2A-myc-Cdc42^{DN} T17N	T17N	↓	Human
au69	*uas*:mCherry-F2A-myc-Cdc42^{DN} F37A	F37A	↓	Xenopus
au70	*uas*:EGFP-F2A-Rac1^{WT}	———	Normal	Human
au72	*uas*:EGFP-F2A-Rac1^{CA}	Q61L	↑	Human
au71	*uas*:EGFP-F2A-Rac1^{DN}	T17N	↓	Human
au73	*uas*:mCherry-F2A-myc-RhoA^{WT}	———	Normal	Human
au75	*uas*:mCherry-F2A-myc-RhoA^{CA}	Q63L	↑	Human
au74	*uas*:mCherry-F2A-myc-RhoA^{DN}	T19N	↓	Human

Fig. 1. Overview of transgenic constructs. **A:** Myc-tagged Cdc42 and RhoA constructs are placed downstream of mCherry and the self-cleaving viral peptide f2a, enabling their bicistronic expression following activation of the 10x*uas* promoter. 10x*uas* activation leads to the bicistronic expression of egfp-f2a and Rac1. Each construct includes *cmlc2:*egfp oriented in reverse orientation **B:** Chart detailing each specific isoform of Rho GTPase, with its predicted activity and species of origin.

Rho GTPase function is dependent upon prenylation at the C-terminus, Rho GTPase sequence could not be placed upstream of the F2A element, as that would have resulted in the C-terminal fusion of the F2A peptide and the disruption of protein trafficking. Thus, to confirm that GAL4-mediated transgene induction results in expression of both the Rho GTPase and the reporter proteins, we performed Western blot analyses of heat-shocked F1 embryos of Cdc42 and RhoA constructs (Fig. 2). GAL4-induced embryos displayed high levels of myc-tagged protein, while no myc-tagged protein was observed in GAL4-negative embryos. This confirms that the F2A peptide is functioning properly by enabling bicistronic expression of mCherry and myc-tagged Rho GTPase protein, both of which are inducible only by GAL4. Western blot analysis of heat-shocked F1 embryos of Rac1 constructs using human Rac1 antibody showed strong Rac1 staining in both GFP^{+} and GFP^{-} siblings, indicating that the Rac1 antibody also detects endogenous Rac1, an unsurprising result considering that human Rac1 protein sequence is 93% identical to zebrafish (data not shown). While expression of all constructs was induced, Cdc42^{F37A} displayed a higher level of expression than the other Cdc42 alleles. One potential explanation for this result is that *Xenopus* Cdc42^{F37A} has greater stability in zebrafish compared to human Cdc42. However, there also appears to be higher expression of mCherry in Cdc42^{F37A} embryos (Fig. 5). Our bicistronic constructs result in the expression of two separate proteins; mCherry should not display any species-dependent enhancement of stability. Tol2 transgenesis often leads to allelic quality differences between founders due to random integration events into the genome; therefore, a more likely explanation is that *uas*:mCherry-f2a-myc-Cdc42^{F37A} is a particularly well expressed allele due to its genomic location.

To confirm that the transgenes are spatially and temporally responsive to GAL4, F0 *uas*:mCherry-f2a-cdc42^{WT} transgenics were crossed to *pou4f3*:gal4, which express GAL4 in a subset (< 20%) of retinal ganglion cells (RGCs) (Xiao and Baier, 2007). To determine if Cdc42 expression is confined to RGCs in the retina, we cryosectioned 4-day-post-fertilization (dpf) transgenic embryos and imaged the retina for mCherry fluorescence (Fig. 3). The mCherry fluorescence is confined to the RGC layer in a pattern consistent with previous studies utilizing the *pou4f3*:gal4

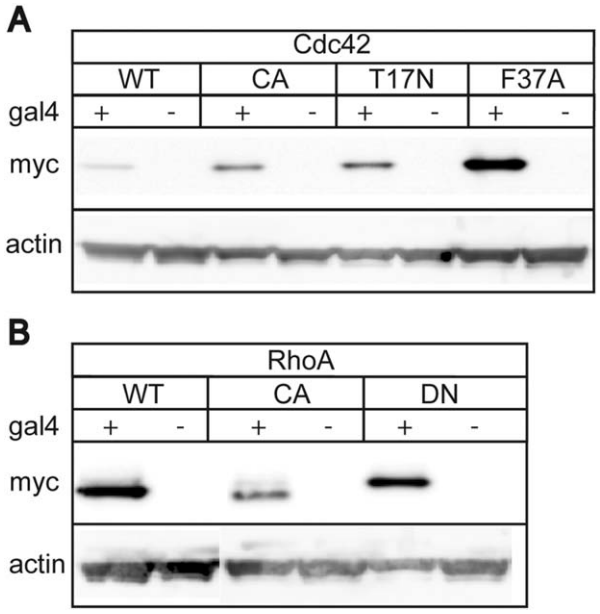

Fig. 2. Induced embryos express myc-tagged protein. **A:** Western blot analysis of myc-tagged Cdc42 and β-actin in *hsp70l*:gal4-positive and -negative Cdc42 transgenic embryos. Myc-labeled protein at the expected size of Cdc42 appears only in gal4-induced embryos. **B:** Western blot analysis of myc-tagged RhoA and β-actin for each RhoA transgenic shows the presence of myc-RhoA only in gal4-induced embryos.

driver (Xiao et al., 2005), indicating that our construct expression is restricted to RGCs and that our transgenic constructs are amenable to cell-specific expression. To determine if cells expressing mCherry also express myc-Rho GTPase, we immunostained for myc in *uas*:mCherry-f2a-myc-Cdc42^{WT} embryos both with and without the *hsp70l*:gal4 transgene. Following heat shock, immunostaining reveals strong induction of both mCherry and myc throughout the retina (Fig. 4A), which is entirely absent in mCherry-negative siblings (Fig. 4B). Next, we crossed *uas*:GFP-f2a-Rac1^{WT} to *ptf1a*:gal4, a driver expressing GAL4 in amacrine cells and horizontal cells (Parsons et al., 2009), and stained retinal sections for human Rac1 (Penzes et al., 2000). Rac1 staining was detected throughout the retina, further supporting our hypothesis that this antibody detects endogenous Rac1. However, there does appear to be a higher degree of Rac1 signal in GFP-positive cells (Fig. 4C), supporting *ptf1a*:gal4-driven cell-specific induction of the construct. Similarly, immunostaining of *hsp70l*:GAL4;*UAS*:mCherry-f2a-RhoA^{WT} showed mCherry and myc colocalization only in mCherry-expressing cells (Fig. 4D,E).

Finally, we sought to validate transgene function by determining whether transgene expression leads to distinct morphological phenotypes. The majority of transgenics heat shocked at 3 dpf did not display an overt phenotype by ~18 hours post–heat shock, with two notable exceptions: Induced Cdc42^{CA} and RhoA^{CA} embryos displayed widespread tissue disorganization and cardiac defects (data not shown). Such phenotypes are not surprising, as RhoA is required for cardiac development in chick (Kaarbø et al., 2003) and has been shown to be critical for proper heart morphogenesis and contractile function (Phillips et al., 2005; Sah et al., 1999), while Cdc42 regulates sarcomere assembly during cardiomyocyte development (Nagai et al., 2003). Because heat shock in these cases occurred late during embryonic development, we reasoned that heat-shocking embryos earlier during development will likely lead to more pronounced phenotypes. Therefore, we heat-shocked F1 transgenics outcrossed to *hsp70l:GAL4*, at ~26 hpf. At 50 hpf, embryos were examined for overt embryonic phenotypes and transgene expression, and then were fixed, sectioned, and stained for F-actin and DAPI to examine the structure of the eye (Figs. 5–7).

While no overt phenotype was detected in Cdc42^{WT} embryos, the lens epithelium was thicker and lens fibers appeared mildly disorganized (Fig. 5A). Cdc42^{CA}-expressing embryos displayed heart defects and edema, and they were microphthalmic. Cryosectioning revealed severe lens fiber disorganization (Fig. 5B). Despite the lack of gross morphological defects in embryos expressing either of the Cdc42^{DN} isoforms, cryosections revealed severe lens fiber disorganization in both (Fig. 5C,D). Rac^{WT}-expressing embryos were microphthalmic, but lens formation appeared largely normal (Fig. 6A). Rac^{CA}-expressing embryos displayed obvious morphological defects, including microphthalmia and cardiac edema, as well as severe disruption of lens fiber organization (Fig. 6B). Rac^{DN}-expressing embryos displayed lower levels of cardiac edema, but sections revealed notable lens fiber disorganization (Fig. 6C). Finally, overexpression of RhoA^{WT} resulted in mild lens fiber disorganization (Fig. 7A). Rho^{CA}-expressing embryos were microphthalmic and possessed heart defects, mild cardiac edema, and severe lens fiber disorganization (Fig. 7B). Embryos expressing Rho^{DN} were also microphthalmic, and lens fibers were disorganized (Fig. 7C).

Cdc42, Rac1, and RhoA are all expressed in the lens (Chen et al., 2006) and have been implicated to play a critical role during lens formation from several studies. For example, knockout of RhoA and Rac1 in the mouse lens disrupts lens development, and defects include disorganization of the lens fibers' actin cytoskeleton (Maddala et al., 2011; Maddala et al., 2004); Cdc42 is required for lens pit invagination and early lens development (Chauhan et al., 2009; Muccioli et al., 2016). Thus, the lens phenotypes detailed here provide strong evidence that our transgenes express functional Rho GTPase proteins. However, it is important to note that numerous additional experiments must still be performed to definitively establish the role of Rho GTPases in lens formation during these developmental windows, as it is equally plausible that the defects reported here arise indirectly from pleiotropic disruption of general embryonic or ocular development following widespread modulation of GTPase function throughout the embryo, and thus do not reflect a direct function of these Rho GTPase proteins during lens development.

These validated transgenic lines represent a versatile tool kit for the temporal-spatial modulation of Cdc42, RhoA, and Rac1 activity. To our knowledge, these are the first UAS-inducible transgenic lines for the bicistronic expression of Rho GTPases and a fluorescent reporter. Furthermore, myc tags on Cdc42 and RhoA allow direct determination of protein expression, as well as potential experiments assaying the altered cellular localization and behaviors of mutant Rho GTPases. However, due to the requirement of GAL4 induction for construct expression and the inherent time delay therein, these transgenic lines are not optimal for studying Rho GTPase function during early developmental processes; their utility lies in modulating Rho GTPase activity during later development, during time points and in tissues that have been inaccessible using previous approaches.

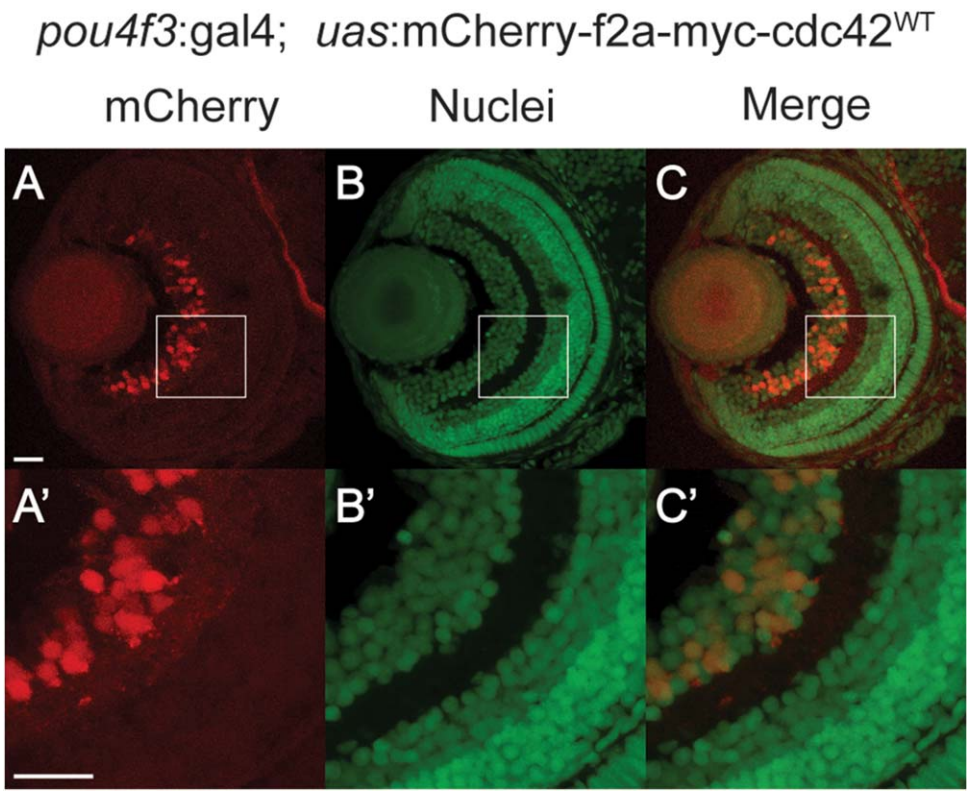

Fig. 3. Tissue-specific control of transgene expression. Driven by *pou4f3*:gal4, mCherry (**A,A′**) is specifically expressed in the RGC layer (**B,B′**) of 4dpf *pou4f3:*gal4;*uas*:mCherry-f2a-Cdc42^{WT} embryos. **A′–C′** are magnified images taken from the boxed regions in **A–C**. Scale bars = 20 μm.

Experimental Procedures

Fish Maintenance and Husbandry

zebrafish were maintained at 28.5°C on a 14-hour-light/10-hour-dark cycle. Embryos were obtained from the natural spawning of transgenic or wild-type parents in pairwise crosses. According to established protocols (Westerfield, 2007), embryos were collected and raised at 28.5°C in the dark until they reached appropriate ages for experimentation. *hsp70l*:gal4^{kca4} (Scheer et al., 2001) transgenic embryos were obtained from the zebrafish International Resource Center (ZIRC) and were propagated by outcrosses to AB-strain wild-type fish. *pou4f3*:gal4^{s311t} transgenic (Xiao and Baier, 2007) embryos were provided by Dr. Chris Chang and propagated by outcrosses to AB-strain fish. *ptf1a*:gal4 transgenic embryos were provided by Dr. Michael Parsons (Johns Hopkins University) and propagated by outcrosses to AB-strain wild-type fish (Parsons et al., 2009). All animals were treated in accordance with provisions established by the University of Texas at Austin and University of Pittsburgh School of Medicine Institutional Animal Care and Use Committees. The following transgenic lines were generated in this study: *au66* (*uas*:mCherry-f2a-myc-Cdc42^{WT}), *au67* (*uas*:mCherry-f2a-myc-Cdc42^{T17N}), *au68* (*uas*:mCherry-f2a-myc-Cdc42^{CA}), *au69* (*uas*:mCherry-f2a-myc-Cdc42^{F37A}), *au70* (*uas*:mcherry-f2a-Rac1^{WT}), *au71* (*uas*:mcherry-f2a-Rac1^{DN}), *au72* (*uas*:mcherry-f2a-Rac1^{CA}), *au73* (*uas*:mCherry-f2a-myc-RhoA^{WT}), *au74* (*uas*:mCherry-f2a-myc-RhoA^{DN}), and *au75* (*uas*:mCherry-f2a-myc-RhoA^{CA}). These will be deposited at ZIRC for distribution.

Assembly of Constructs

Constructs encoding human and *Xenopus* Cdc42, Rac1, and RhoA were provided by Dr. John Wallingford (Kieserman and Wallingford, 2009; Nobes and Hall, 1995; Sokol et al., 2001).

Cdc42: To create pME-mCherry-f2a-Cdc42^{wt} (pME-mCWT), a pUCIDT-attL1-mCherry-f2a-myc-Cdc42^{wt}-attL2 (pUCIDT-mCWT) oligo was purchased from IDT Gene Synthesis and used to create a pME-mCherry-f2a-Cdc42^{WT} via Gateway cloning (Invitrogen). To build pME-mCherry-f2a-myc-Cdc42^{CA} (pME-mCCA), pME-mCherry-f2a-myc-Cdc42^{DN}(T17N) (pME-mCDN), and pME-mCherry-f2a-myc-Cdc42^{DN}(F37A) (pME-mCF37A), each Cdc42 isoform was PCR-amplified from pCS2+Cdc42^{XX} plasmids using primers 3 and 4 (Table 1) to create Cdc42^{xx}-attL2 PCR fragments. attL1-mCherry-f2a was PCR-amplified from pUCIDT-attL1-mCherry-f2a-Cdc42^{WT}-attL2 using primers 4 and 5 (Table 1). These PCR fragments were then cloned into pME via Gibson Assembly (New England Biolabs).

LR Clonase II Plus was used to carry out all MultiSite Gateway assembly reactions using protocols established previously (Kwan et al., 2007). Tg(*uas*:mCherry-f2a-myc-Cdc42^{XX}) was created using Tol2Kit vectors #302 (p3E-pA), #327 (p5E-UAS), #395 (pDestTol2CG), and pME-mCXX.

RhoA: To build pME-mCherry-f2a-myc-RhoA^{WT} (pME-mRhWT), pME-mCherry-f2a-myc-RhoA^{CA} (pME-mRhCA), and pME-mCherry-f2a-myc-RhoA^{DN} (pME-mRhDN), each RhoA isoform was PCR-amplified from pCS2+RhoA^{XX} plasmids using primers 5 and 6 (Table 1) to create RhoA^{xx}-attL2 PCR fragments. attL1-mCherry-f2a was PCR-amplified from pUCIDT-mCWT using primers 4 and 5 (Table 1). These PCR fragments were then cloned into pME via Gibson Assembly (New England Biolabs).

Tg(uas:mCherry-f2a-myc-RhoA2^{XX}) was created using Tol2Kit vectors #302 (p3E-pA), #327 (p5E-UAS), #395 (pDestTol2CG), and pME-mRhXX.

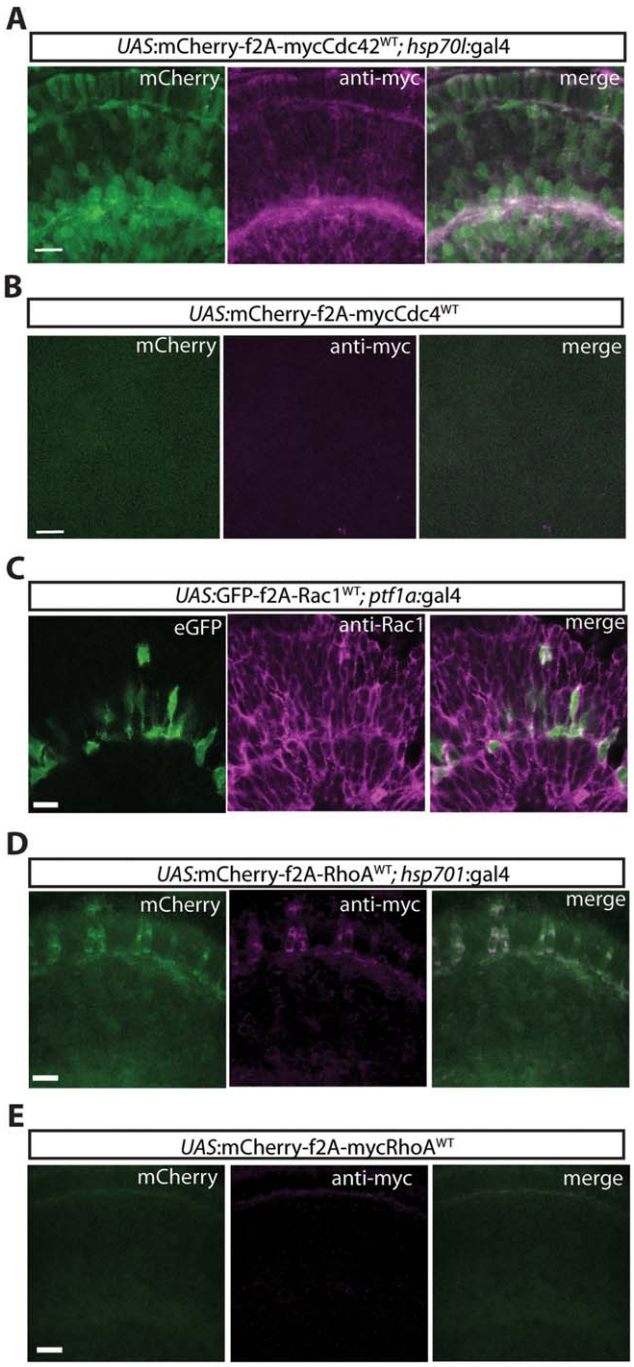

Fig. 4. Antibody validation of transgene expression. **A:** Myc colocalization with mCherry expression in heat-shocked *hsp70l*:gal4;*uas*:mCherry-F2A-myc-Cdc42^{WT} embryos. **B:** No signal for mCherry or myc was detected in *uas*:mCherry-F2A-myc-Cdc42^{WT} transgenics missing the *hsp70l*:gal4 transgene. **C:** Rac1 antibody staining in *ptf1a*:gal4;*uas*:gfp-f2a-Rac1^{WT} embryos. **D:** Myc colocalization with mCherry expression in heat-shocked *hsp70l*:gal4;*uas*:mCherry-F2A-myc-RhoA^{WT} retinae. **E:** No signal for mCherry or myc was detected in *uas*:mCherry-F2A-myc-RhoA^{WT} transgenics missing the *hsp70l:*gal4 transgene. Scale bar = 10μm.

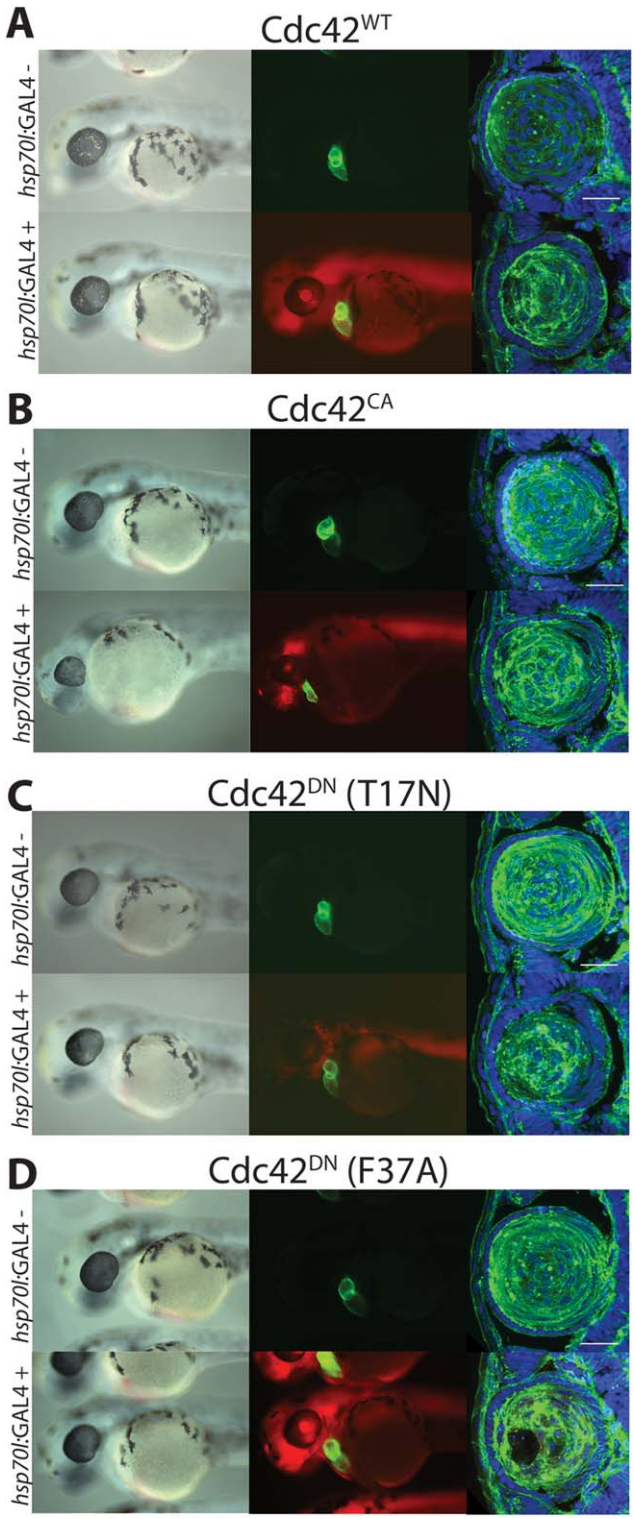

Fig. 5. Construct expression and phenotypes of GAL4-positive and -negative embryos of Cdc42 transgenics. Transgenic F1s were outcrossed to *hsp70l:gal4* zebrafish, and *cmlc2:*egfp^{+} embryos were heat-shocked at ~26 hpf and imaged at ~50 hpf. Gross morphology, transgene expression, and lens structure of *hsp70l:*gal4-positive and -negative **(A)** Cdc42^{WT}, **(B)** Cdc42^{CA} **(C)** Cdc42^{T17N}, and **(D)** Cdc42^{F37A} embryos. Transgene expression was strong and ubiquitous following heat shock, and cryosections reveal lens fiber organization defects in all induced transgenics. Scale bar = 25μm.

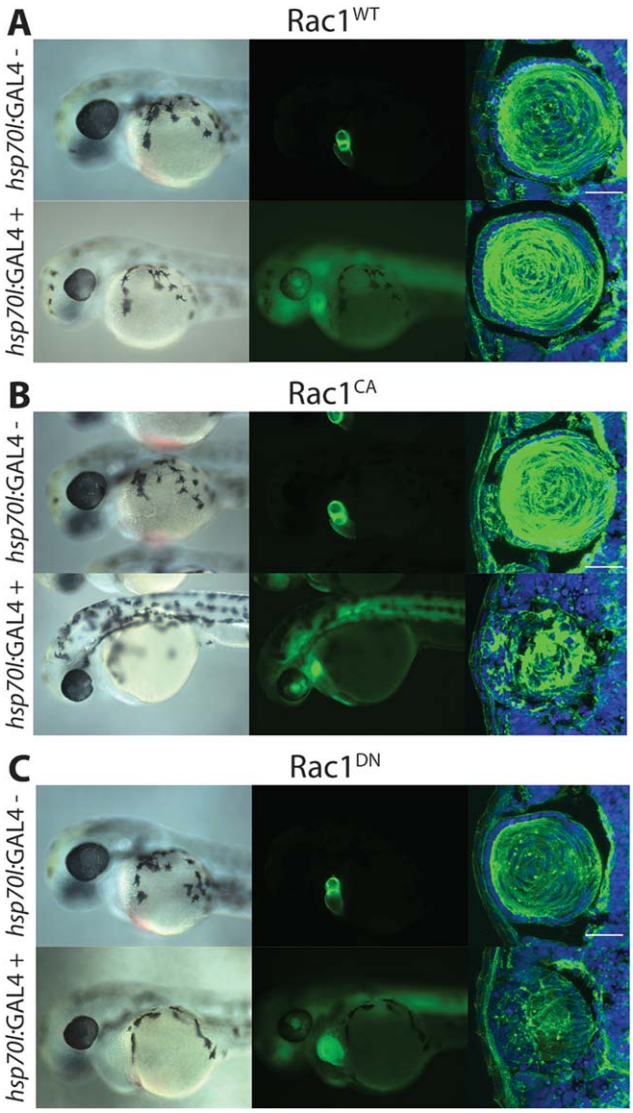

Fig. 6. Construct expression and phenotypes of GAL4-positive and -negative embryos of Rac transgenics. Transgenic F1s were outcrossed to *hsp70l:gal4* zebrafish, and *cmlc2:*egfp^{+} embryos were heat-shocked at ~26 hpf and imaged at ~50 hpf. Gross morphology, transgene expression, and lens structure of *hsp70l:*gal4-positive and -negative **(A)** Rac1^{WT}, **(B)** Rac1^{CA}, and **(C)** Rac1^{DN} embryos. Transgene expression was strong and ubiquitous following heat shock, and cryosections reveal lens fiber organization defects in Rac^{CA} and Rac^{DN} induced transgenics. Scale bar = 25μm.

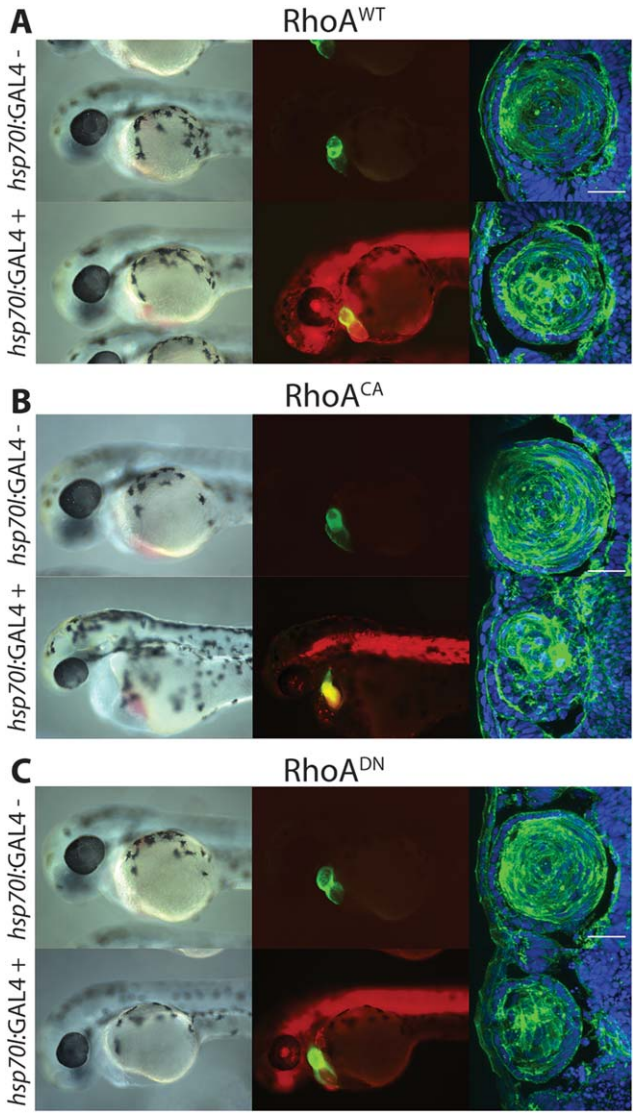

Fig. 7. Construct expression and phenotypes of GAL4-positive and -negative embryos of Rho transgenics. Transgenic F1s were outcrossed to *hsp70l:gal4* zebrafish, and *cmlc2:*egfp^{+} embryos were heat-shocked at ~26 hpf and imaged at ~50 hpf. Gross morphology, transgene expression, and lens structure of *hsp70l:*gal4-positive and -negative **(A)** RhoA^{WT}, **(B)** RhoA^{CA}, and **(C)** RhoA^{DN} embryos. Transgene expression was strong and ubiquitous following heat shock, and cryosections reveal lens fiber organization defects in all induced transgenics. Scale bar = 25μm.

Rac1: To create pME-gfp-f2a-Rac1^{WT} (pME-gRWT) and pME-gfp-f2a-Rac1^{DN} (pME-gRDN), Rac1WT and Rac1DN were PCR-amplified using Vent Polymerase (New England Biolabs) using primers 7 and 8 (Table 1). gfp-f2a was amplified from T2Kactb2:gfp-f2a-creER^{T2} (Wang et al., 2011), a gift from Dr. Michael Parsons, using primers 9 and 10 (Table 1) and cloned into a 3′ entry vector via In-Fusion recombination technology (Clontech). Finally, attB1-egfp-2a-Rac1^{WT}-attB2 and attB1-egfp-2a-Rac1^{DN}-attB2 were amplified via Phusion Polymerase using primers 11 and 14 (Table 1) and recombined with pDONR221 to create middle-entry vectors pME-gRWT and pME-gRDN. To create pME-gfp-f2a-Rac1^{CA} (pME-gRCA), Rac1CA-attB2 was PCR-amplified with Phusion Polymerase using primers 11 and 12 (Table 1) and ligated to attB1-gfp-f2a (primers 13 and 14 [Table 1]) via overlap PCR to form attB1-gfp-f2a-Rac1^{XX}-attB2 PCR fragments. These fragments were then cloned into middle-entry vectors by BP reaction to create pME-gRCA. Tg(*uas*:mCherry-f2a- Rac1^{XX}) constructs were created using Tol2Kit vectors #302 (p3E-pA), #327 (p5E-UAS), #395 (pDest-Tol2CG), and pME-gRXX.

All plasmids were sequence-confirmed via sequencing on Applied Biosystems 3730 DNA Analyzers at the University of Texas at Austin Institute for Cellular and Molecular Biology DNA Sequencing Facility.

Tol2 transgenesis

Capped Tol2 mRNA was synthesized from pCS2FA-transposase using the Ambion mMessage mMachine SP6 in vitro

TABLE 1. Primers Used for Construct Assembly

Primer number	Primer name	Sequence
1	Gibson1 attL1-Not1-Kozak-mCherry FWD	GCCAACTTTGTACAAAAAAGCAGGCTTTGCGG CCGCGCCGCCACCATGGTGAG
2	Gibson1 attL2-Not1-Cdc42 REV	GCCAACTTTGTACAAGAAAGCTGGGTCGCCGC GCTCATAGCAGCACACACCTGC
3	Gibson1 attL2-Not1-RhoA REV	GCCAACTTTGTACAAGAAAGCTGGGTCGCGGC CGCTCACAAGACAAGGCAACCAG
4	Gibson1 attL2-Not1-F37A REV	GCCAACTTTGTACAAGAAAGCTGGGTCGCGGC CGCTCATAGCAGCATACACTTGCGTTTC
5	Gibson2 attL1 REV	AAAGCCTGCTTTTTTGTACAAAGTTGGC
6	Gibson2 attL2 FWD	GACCCAGCTTTCTTGTACAAAGTTGGC
7	Linker-Rac1 FWD	ATGTCCAATTTACTGATGCAGGCCATCAAGTGTGT
8	Rac1 p3pA REV	TATCATGTCTGGATCCTTACAACAGCAGGCATTTTCTCTTCC
9	p3pA-GFP FWD	ACAAAGTGGGGGATCCATGGTGAGCAAGGGCGAG
10	2A-Linker REV	CAGTAAATTGGACATGGGCCCTG
11	attB1-GFP-2a-Linker-Rac REV	CCACACACTTGATGGCCTGCATCAGTAAATTGGACAT GGGCCCTGGGTTG
12	GFP2aCdcWT+Kozak+att FWD	GGGGACAAGTTTGTACAAAAAAGCAGGCTTTGGCCGCC ACCATGGTGAGCAAGGGCGAG
13	GFP-2a-Linker Rac FWD	CAACCCAGGGCCCATGTCCAATTTACTGATGCAGGCCAT CAAGTGTGTGG
14	attB2-Rac1 REV	GGGGACCACTTTGTACAAGAAAGCTGGGTCTTACAACAG CAGGCATTTTCTCTTCC

transcription kit. Between 50 and 75 pg Tol2 mRNA and between 20 and 25 pg cDNA were microinjected into single-cell embryos. Embryos displaying acceptable levels of mosaic *cmlc2*:egfp expression were raised to adulthood and outcrossed to screen for founders. F1 embryos displaying ubiquitous *cmlc2*:egfp expression were isolated and reared to generate stable lines.

Heat shock induction of GAL4

Embryos from *hsp70l*:gal4 outcrosses of transgenic founders were raised in system water supplemented with Phenylthiourea (PTU). Embryos were individually placed in ~120 uL system water in PCR tubes and heat-shocked for 30 minutes at 39.5°C in a PCR thermocycler. They were then immediately returned to 28.5°C fish medium for recovery and imaging on either a Leica MZ16F or a Zeiss Axio Zoom V16 fluorescent stereoscope.

Western blot analysis

Heat-shocked and dechorionated embryos were collected at 3 dpf. To deyolk embryos, a borosilicate injection needle was used to mechanically disrupt yolks. Embryos were next washed in deyolking buffer without calcium (Link et al., 2006), spun at 300 rcf, and washed in wash buffer (110mM NaCl, 3.5mM KCl, 2.7mM $CaCl_2$, 10mM Tris/Cl) containing cOmplete Mini Protease Inhibitor Mixture (Roche Diagnostics). Deyolked embryos were lysed with modified Lemeer's Lysis Buffer (50mM Tris pH 7.5, 150mM NaCl, 1mM EDTA, 1% IGEPAL, 0.1% sodium deoxycholate) supplemented with cOmplete Mini Protease Inhibitor Cocktail (Lemeer et al., 2007) before being centrifuged at low speed and sonicated by a Sonic Dismembrator Model 300 (Fisher Scientific). Using manufacturer's protocol, protein samples were gel-electrophoresed using 4%–12% Bis-Tris gel and transferred onto PVDF membrane (Invitrogen NuPAGE system). Blots were incubated 1:5000 anti-myc (abcam ab9106), followed by 1:5000 horse anti-mouse HRP secondary (Cell Signaling Technology 7076). Blots were imaged via the SuperSignal West Femto visualization system (Life Sciences) on an ImageQuant LAS 4000 machine (GE Life Sciences). Following imaging of myc antibody labeling, blots were stripped for 15 minutes in Restore Western Blot Stripping Buffer (Thermo Scientific 21059) and reprobed with 1:5000 anti-actin (Calbiochem CP01).

Immunohistochemistry of retinal sections

Embryos were fixed in 4% paraformaldehyde overnight at 4°C, sucrose-protected, and embedded in OCT tissue-freezing medium (TBS, Inc.) before being sectioned at 14μm on a Leica CM1850 cryostat. Sections were rehydrated in 1XPBS for 5 minutes and blocked in 5% normal goat serum in PBS for 2 hours at room temperature. Sections were stained with 1:500 TOPRO or 1:500 DAPI (Life Technologies) for nine minutes at room temperature, washed 3X with PBS, and mounted with Vectashield (Vector Laboratories). Images were obtained with a 63X objective on a Leica SP5 confocal microscope. Antibodies used in this study include Rac1 (Millipore, 05-389) and myc (Abcam, ab9106). Phalloidin (Thermo Fisher, A22284) was used at a 1:33 dilution.

Acknowledgments

We thank members of the Gross Lab and Dr. Steve Ekker for helpful comments and suggestions on this work; Ryoko Minowa for fish maintenance; and Phil Anselmo and Nick Cave for technical assistance. This work was supported by NIH RO1 EY18005 to J.M.G.; NIH CORE Grant P30 EY08098 to the Department of Ophthalmology at the University of Pittsburgh School of Medicine; and a Knights Templar Pediatric Ophthalmology Fellowship to E.M. zebrafish were obtained from ZIRC, which is supported by NIH-NCRR Grant P40 RR012546. We acknowledge additional support

from the Eye and Ear Foundation of Pittsburgh and from an unrestricted grant from Research to Prevent Blindness, New York, NY.

References

Adams A, Johnson D, Longnecker R, Sloat B, Pringle J. 1990. CDC42 and CDC43, two additional genes involved in budding and the establishment of cell polarity in the yeast Saccharomyces cerevisiae. J Cell Biol 111:131–142.

Akitake CM, Macurak M, Halpern ME, Goll MG. 2011. Transgenerational analysis of transcriptional silencing in zebrafish. Dev Biol 352:191–201.

Bashaw GJ, Klein R. 2010. Signaling from axon guidance receptors. Cold Spring Harb Perspect Biol 2:a001941.

Boguski M, McCormick F. 1993. Proteins regulating Ras and its relatives. Nature 366:643–654.

Bosco EE, Mulloy JC, Zheng Y. 2009. Rac1 GTPase: a "Rac" of all trades. Cell Mol Life Sci 66:370–374.

Brand A, Perrimon N. 1993. Targeted gene expression as a means of altering cell fates and generating dominant phenotypes. Development 415:401–415.

Chan HY, V S, Xing X, Kraus P, Yap SP, Ng P, Lim SL, Lufkin T. 2011. Comparison of IRES and F2A-based locus-specific multicistronic expression in stable mouse lines. PLoS One 6;e28885.

Chauhan BK, Disanza A, Choi S-Y, Faber SC, Lou M, Beggs HE, Scita G, Zheng Y, Lang RA. 2009. Cdc42- and IRSp53-dependent contractile filopodia tether presumptive lens and retina to coordinate epithelial invagination. Development 136:3657–3667.

Chen F, Ma L, Parrini M, Mao X, Lopez M. 2000. Cdc42 is required for PIP 2-induced actin polymerization and early development but not for cell viability. Curr Biol 10:758–765.

Chen Y, Stump RJW, Lovicu FJ, McAvoy JW. 2006. A role for Wnt/planar cell polarity signaling during lens fiber cell differentiation? Semin Cell Dev Biol 17:712–725.

Chew TW, Liu XJ, Liu L, Spitsbergen JM, Gong Z, Low BC. 2014. Crosstalk of Ras and Rho: activation of RhoA abates Kras-induced liver tumorigenesis in transgenic zebrafish models. Oncogene 33;2717–2727.

Choe CP, Collazo A, Trinh le A, Pan L, Moens CB, Crump JG. 2013. Wnt-dependent epithelial transitions drive pharyngeal pouch formation. Dev Cell 24:296–309.

Choe S-K, Nakamura M, Ladam F, Etheridge L, Sagerström CG. 2012. A Gal4/UAS system for conditional transgene expression in rhombomere 4 of the zebrafish hindbrain. Dev Dyn 241:1125–1132.

Disanza A, Mantoani S, Hertzog M, Gerboth S, Frittoli E, Steffen A, Berhoerster K, Kreienkamp H-J, Milanesi F, Di Fiore PP, Ciliberto A, Stradal TEB, Scita G. 2006. Regulation of cell shape by Cdc42 is mediated by the synergic actin-bundling activity of the Eps8-IRSp53 complex. Nat Cell Biol 8:1337–1347.

Donnelly M, Luke G. 2001. Analysis of the aphthovirus 2A/2B polyprotein "cleavage"mechanism indicates not a proteolytic reaction, but a novel translational effect: a putative ribosomal "skip." J Gen Virol 82:1013–1025.

Ellenbroek SIJ, Collard JG. 2007. Rho GTPases: functions and association with cancer. Clin Exp Metastasis 24:657–672.

Erickson JW, Cerione RA. 2001. Multiple roles for Cdc42 in cell regulation. Curr Opin Cell Biol 13:153–157.

Etienne-Manneville S, Hall A. 2002. Rho GTPases in cell biology. Nature 420:629–635.

Fischer J, Giniger E, Maniatis T, Ptashne M. 1988. GAL4 activates transcription in Drosophila. Nature 332:853–856.

Gabriel J, Trivedi C, Maurer C. 2012. Layer-Specific Targeting of Direction Selective Neurons in the zebrafish Optic Tectum. Neuron 76:1147–1160.

Goll MG, Anderson R, Stainier DYR, Spradling AC, Halpern ME. 2009. Transcriptional silencing and reactivation in transgenic zebrafish. Genetics 182:747–755.

Govek E, Newey S, Van Aelst L. 2005. The role of the Rho GTPases in neuronal development. Genes Dev 19:1–49.

Hall A. 1998. Rho GTPases and the Actin Cytoskeleton. Science 279:509–514.

Heasman SJ, Ridley AJ. 2008. Mammalian Rho GTPases: new insights into their functions from in vivo studies. Nat Rev Mol Cell Biol 9:690–701.

Heynen SR, Meneau I, Caprara C, Samardzija M, Imsand C, Levine EM, Grimm C. 2013. CDC42 is required for tissue lamination and cell survival in the mouse retina. PLoS One 8:e53806.

Hsu CL, Muerdter CP, Knickerbocker AD, Walsh RM, Zepeda-Rivera MA, Depner KH, Sangesland M, Cisneros TB, Kim JY, Sanchez-Vazquez P, Cherezova L, Regan RD, Bahrami NM, Gray EA, Chan AY, Chen T, Rao MY, Hille MB. 2012. Cdc42 GTPase and Rac1 GTPase act downstream of p120 catenin and require GTP exchange during gastrulation of zebrafish mesoderm. Dev Dyn 241:1545–1561.

Hussain NK, Jenna S, Glogauer M, Quinn CC, Wasiak S, Guipponi M, Antonarakis SE, Kay BK, Stossel TP, Lamarche-Vane N, McPherson PS. 2001. Endocytic protein intersectin-l regulates actin assembly via Cdc42 and N-WASP. Nat Cell Biol 3:927–932.

Jackson B, Peyrollier K, Pedersen E, Basse A, Karlsson R, Wang Z, Lefever T, Ochsenbein AM, Schmidt G, Aktories K, Stanley A, Quondamatteo F, Ladwein M, Rottner K, van Hengel J, Brakebusch C. 2011. RhoA is dispensable for skin development, but crucial for contraction and directed migration of keratinocytes. Mol Biol Cell 22:593–605.

Jaffe AB, Hall A. 2005. Rho GTPases: biochemistry and biology. Annu Rev Cell Dev Biol 21:247–269.

Jin M, Guan C, Jiang Y, Chen G, Zhao C, Cui K, Song Y, Wu C, Poo M, Yuan X. 2005. Ca2+-dependent regulation of rho GTPases triggers turning of nerve growth cones. J Neurosci 25:2338–2347.

Jung I, Leem G. 2013. Glioma is formed by active Akt1 and promoted by active Rac1 in transgenic zebrafish. Neuro Oncol 15: 290–304.

Kaarbø M, Crane DI, Murrell WG. 2003. RhoA is highly upregulated in the process of early heart development of the chick and important for normal embryogenesis. Dev Dyn 227:35–47.

Kardash E, Reichman-Fried M, Maître J-L, Boldajipour B, Papusheva E, Messerschmidt E-M, Heisenberg C-P, Raz E. 2010. A role for Rho GTPases and cell-cell adhesion in single-cell motility in vivo. Nat Cell Biol 12:47–53.

Kieserman EK, Wallingford JB. 2009. In vivo imaging reveals a role for Cdc42 in spindle positioning and planar orientation of cell divisions during vertebrate neural tube closure. J Cell Sci 122: 2481–2490.

Kim G-H, Her J-H, Han J-K 2008. Ryk cooperates with Frizzled 7 to promote Wnt11-mediated endocytosis and is essential for Xenopus laevis convergent extension movements. J Cell Biol 182:1073–1082.

Kroschewski R, Hall A, Mellman I. 1999. Cdc42 controls secretory and endocytic transport to the basolateral plasma membrane of MDCK cells. Nat Cell Biol 1:8–13.

Kwan KM, Fujimoto E, Grabher C, Mangum BD, Hardy ME, Campbell DS, Parant JM, Yost HJ, Kanki JP, Chien C-B. 2007. The Tol2kit: a multisite gateway-based construction kit for Tol2 transposon transgenesis constructs. Dev Dyn 236:3088–3099.

Lai S-L, Chang C-N, Wang P-J, Lee S-J. 2005. Rho mediates cytokinesis and epiboly via ROCK in zebrafish. Mol Reprod Dev 71: 186–196.

Lee YN, Malbon CC, Wang HY. 2004. Ga13 signals via p115RhoGEF cascades regulating JNK1 and primitive endoderm formation. J Biol Chem 279:54896–54904.

Lemeer S, Ruijtenbeek R, Pinkse MWH, Jopling C, Heck AJR, den Hertog J, Slijper M. 2007. Endogenous phosphotyrosine signaling in zebrafish embryos. Mol Cell Proteomics 6:2088–2099.

Link V, Shevchenko A, Heisenberg C-P. 2006. Proteomics of early zebrafish embryos. BMC Dev Biol 6:1.

Luo L. 2002. Actin cytoskeleton regulation in neuronal morphogenesis and structural plasticity. Annu Rev Cell Dev Biol 18:601–635.

Luo L, Hensch T, Ackerman L, Barbel S. 1996. Differential effects of the Rac GTPase on Purkinje cell axons and dendritic trunks and spines. Nature 379:837–840.

Maddala R, Chauhan BK, Walker C, Zheng Y, Robinson ML, Lang RA, Rao PV. 2011. Rac1 GTPase-deficient mouse lens exhibits defects in shape, suture formation, fiber cell migration and survival. Dev Biol 360:30–43.

Maddala R, Deng P-F, Costello JM, Wawrousek EF, Zigler JS, Rao VP. 2004. Impaired cytoskeletal organization and membrane integrity in lens fibers of a Rho GTPase functional knockout transgenic mouse. Lab Invest 84:679–692.
Muccioli M, Qaisi D, Herman K, Plageman TF. 2016. Lens placode planar cell polarity is dependent on Cdc42-mediated junctional contraction inhibition. Dev Biol 412:32–43.
Nagai T, Tanaka-Ishikawa M, Aikawa R, Ishihara H, Zhu W, Yazaki Y, Nagai R, Komuro I. 2003. Cdc42 plays a critical role in assembly of sarcomere units in series of cardiac myocytes. Biochem Biophys Res Commun 305:806–810.
Nobes CD, Hall A. 1995. Rho, Rac, and Cdc42 GTPases regulate the assembly of multimolecular focal complexes associated with actin stress fibers, lamellipodia, and filopodia. Cell 81:53–62.
Olson M, Ashworth A, Hall A. 1995. An essential role for Rho, Rac, and Cdc42 GTPases in cell cycle progression through G1. Science 269:1270–1272.
Ornitz DM, Moreadith RW, Leder P. 1991. Binary system for regulating transgene expression in mice: Targeting int-2 gene expression with yeast GAL4 / UAS control elements. Proc Natl Acad Sci U S A 88:698–702.
Parsons MJ, Pisharath H, Yusuff S, Moore JC, Siekmann AF, Lawson N, Leach SD. 2009. Notch-responsive cells initiate the secondary transition in larval zebrafish pancreas. Mech Dev 126: 898–912.
Penzes P, Johnson RC, Alam MR, Kambampati V, Mains RE, Eipper BA. 2000. An isoform of kalirin, a brain-specific GDP/GTP exchange factor, is enriched in the postsynaptic density fraction. J Biol Chem 275:6395–6403.
Phillips HM, Murdoch JN, Chaudhry B, Copp AJ, Henderson DJ. 2005. Vangl2 acts via RhoA signaling to regulate polarized cell movements during development of the proximal outflow tract. Circ Res 96:292–299.
Piekny A, Werner M, Glotzer M. 2005. Cytokinesis: Welcome to the Rho zone. Trends Cell Biol 15:651–658.
Raftopoulou M, Hall A. 2004. Cell migration: Rho GTPases lead the way. Dev Biol 265:23–32.
Ridley A, Paterson H, Johnston C. 1992. The Small GTP-Binding Protein rac Regulates Growth Factor-Induced Membrane. Cell 70:401–410.
Ruchhoeft M, Ohnuma S. 1999. The neuronal architecture of Xenopus retinal ganglion cells is sculpted by rho-family GTPases in vivo. J Neurosci 19:8454–8463.
Sah VP, Minamisawa S, Tam SP, Wu TH, Dorn GW, Ross J, Chien KR, Brown JH. 1999. Cardiac-specific overexpression of RhoA results in sinus and atrioventricular nodal dysfunction and contractile failure. J Clin Invest 103:1627–1634.
Sahai E, Marshall CJ. 2002. RHO-GTPases and cancer. Nat Rev Cancer 2:133–142.
Sakurai-Yageta M, Recchi C, Le Dez G, Sibarita JB, Daviet L, Camonis J, D'Souza-Schorey C, Chavrier P. 2008. The interaction of IQGAP1 with the exocyst complex is required for tumor cell invasion downstream of Cdc42 and RhoA. J Cell Biol 181: 985–998.
Salas-Vidal E, Meijer AH, Cheng X, Spaink HP. 2005. Genomic annotation and expression analysis of the zebrafish Rho small GTPase family during development and bacterial infection. Genomics 86:25–37.
Scheer N. 1999. Use of the Gal4-UAS technique for targeted gene expression in the zebrafish. Mech Dev 80:153–158.
Scheer N, Groth A, Hans S, Campos-Ortega J. 2001. An instructive function for Notch in promoting gliogenesis in the zebrafish retina. Development 1107:1099–1107.
Shaner NC, Campbell RE, Steinbach PA, Giepmans BNG, Palmer AE, Tsien RY. 2004. Improved monomeric red, orange and yellow fluorescent proteins derived from Discosoma sp. red fluorescent protein. Nat Biotechnol 22:1567–1572.
Sokol SY, Li Z, Sacks DB. 2001. The effect of IQGAP1 on Xenopus embryonic ectoderm requires Cdc42. J Biol Chem 276:48425–48430.
Srinivas BP, Woo J, Leong WY, Roy S. 2007. A conserved molecular pathway mediates myoblast fusion in insects and vertebrates. Nat Genet 39:781–786.
Sugihara K, Nakatsuji N, Nakamura K. 1998. Rac1 is required for the formation of three germ layers during gastrulation. Oncogene 17:3427–3433.
Szymczak AL, Workman CJ, Wang Y, Vignali KM, Dilioglou S, Vanin EF, Vignali DA. 2004. Correction of multi-gene deficiency in vivo using a single "self-cleaving" 2A peptide-based retroviral vector. Nat Biotechnol 22:589–594.
Takai Y, Sasaki T, Matozaki T. 2001. Small GTP-binding proteins. Physiol Rev 81:153–208.
Wang Y, Rovira M, Yusuff S, Parsons MJ. 2011. Genetic inducible fate mapping in larval zebrafish reveals origins of adult insulin-producing β-cells. Development 138:609–617.
Westerfield, M. 2007. The Zebrafish Book, 5th Edition: A guide for the laboratory use of zebrafish (Danio rerio), Eugene, University of Oregon Press.
Wong W, Faulkner-Jones B. 2000. Rapid dendritic remodeling in the developing retina: dependence on neurotransmission and reciprocal regulation by Rac and Rho. J Neurosci 20:5024–5036.
Xiang S, Vanhoutte D. 2011. RhoA protects the mouse heart against ischemia/reperfusion injury. J Clin Invest 121:3269–3276.
Xiao T, Baier H. 2007. Lamina-specific axonal projections in the zebrafish tectum require the type IV collagen Dragnet Nat Neurosci 10:1529–1537.
Xiao T, Roeser T, Staub W, Baier H. 2005. A GFP-based genetic screen reveals mutations that disrupt the architecture of the zebrafish retinotectal projection. Development 132:2955–2967.
Xu X, Shuen WH, Chen C, Goudevenou K, Jones P, Sablitzky F. 2014. Swap70b is required for convergent and extension cell movement during zebrafish gastrulation linking Wnt11 signalling and RhoA effector function. Dev Biol 386:191–203.
Yeh C-M, Liu Y-C, Chang C-J, Lai S-L, Hsiao C-D, Lee S-J. 2011. Ptenb mediates gastrulation cell movements via Cdc42/AKT1 in zebrafish. PLoS One 6:e18702.
Zhu S, Korzh V, Gong Z, Low BC. 2008. RhoA prevents apoptosis during zebrafish embryogenesis through activation of Mek/Erk pathway. Oncogene 27:1580–1589.
Zhu S, Liu L, Korzh V, Gong Z, Low BC. 2006. RhoA acts downstream of Wnt5 and Wnt11 to regulate convergence and extension movements by involving effectors Rho kinase and Diaphanous: use of zebrafish as an in vivo model for GTPase signaling. Cell Signal 18:359–372.